Mon. Not. R. Astron. Soc. **396,** 2228–2236 (2009) doi:10.1111/j.1365-2966.2009.14879.x

# Time-dependent models of the structure and stability of self-gravitating protoplanetary discs

W. K. M. Rice[1⋆] and Philip J. Armitage[2,3]

[1]*Scottish Universities Physics Alliance (SUPA), Institute for Astronomy, University of Edinburgh, Blackford Hill, Edinburgh EH9 3HJ*
[2]*JILA, Campus Box 440, University of Colorado, Boulder, CO 80309, USA*
[3]*Department of Astrophysical and Planetary Sciences, University of Colorado, Boulder, CO 80309, USA*

Accepted 2009 April 7. Received 2009 March 24; in original form 2009 February 16

**ABSTRACT**

Angular momentum transport within young massive protoplanetary discs may be dominated by self-gravity at radii where the disc is too weakly ionized to allow the development of the magneto-rotational instability. We use time-dependent one-dimensional disc models, based on a local cooling time calculation of the efficiency of transport, to study the radial structure and stability (against fragmentation) of protoplanetary discs in which self-gravity is the sole transport mechanism. We find that self-gravitating discs rapidly attain a quasi-steady state in which the surface density in the inner disc is high and the strength of turbulence very low ($\alpha \sim 10^{-3}$ or less inside 5 au). Temperatures high enough to form crystalline silicates may extend out to several astronomical units at early times within these discs. None of our discs spontaneously develop regions that would be unambiguously unstable to fragmentation into substellar objects, though the outer regions (beyond 20 au) of the most massive discs are close enough to the threshold that fragmentation cannot be ruled out. We discuss how the mass accretion rates through such discs may vary with disc mass and with mass of the central star, and note that a determination of the $\dot{M}$–$M_*$ relation for very young systems may allow a test of the model.

**Key words:** circumstellar matter – stars: formation – planetary systems: formation – planetary systems: protoplanetary discs – stars: pre-main-sequence.

## 1 INTRODUCTION

Low-mass stars form from the collapse of cold, dense molecular cloud cores (Terebey, Shu & Cassen 1984). Although the rotation rates of such cores are generally quite small (Caselli et al. 2002), they none the less contain amounts of angular momentum far in excess of the rotational angular momentum of a single star. Most of the mass must therefore pass through a protostellar disc, and the answers to many open problems in star and planet formation hinge on the nature of the angular momentum transport that is needed for disc accretion.

In most astrophysical discs, the fundamental question of what mechanism dominates angular momentum transport is widely considered to have been solved – magnetohydrodynamic (MHD) turbulence initiated by the magneto-rotational instability (MRI) can provide the necessary viscosity (Balbus & Hawley 1991; Papaloizou & Nelson 2003). Protoplanetary discs, however, are so cold and dense that thermal processes probably fail to yield even the very small degree of ionization needed to sustain MHD turbulence (Blaes & Balbus 1994). Under these conditions disc self-gravity may provide an alternate and possibly dominant mechanism for transporting angular momentum through the growth of the gravitational instability (Toomre 1964; Lin & Pringle 1987; Laughlin & Bodenheimer 1994).

Study of the development of gravitational instability in protostellar discs has often been motivated largely by the possibility that the instability will lead to fragmentation of the disc and the formation of gas giant planets (Boss 1998). The conditions for fragmentation are, however, quite difficult to achieve, especially in the inner, planet-forming regions (Matzner & Levin 2005; Rafikov 2005; Boley et al. 2006; Whitworth & Stamatellos 2006; Stamatellos & Whitworth 2008; Forgan et al. 2009). What seems more likely is that discs will evolve towards quasi-steady states in which the instability acts to transport angular momentum outwards (Gammie 2001; Rice et al. 2003; Lodato & Rice 2004; Vorobyov & Basu 2007). This is of interest in its own right, as it implies that the conditions within young protoplanetary discs – at precisely the epoch when planetesimals and perhaps larger bodies are forming – may largely be set by the physics of angular momentum transport via gravitational instability. The recent progress in understanding the conditions for fragmentation has yielded a much clearer understanding of this physics,

⋆E-mail: wkmr@roe.ac.uk

which we use here to construct realistic time-dependent models for the structure of self-gravitating protoplanetary discs. Our models rely on two specific properties of transport via gravitational instability. First, that transport can be approximated as a local viscous process for all except the most massive discs (Lodato & Rice 2004, 2005). Second, under conditions of thermal equilibrium, the strength of angular momentum transport is set by the cooling rate of the disc (Gammie 2001; Rice et al. 2003). Our results show that self-gravitating discs will settle into quasi-steady states that appear independent of the initial conditions, but that their properties are quite unlike those that result from angular momentum transport via generic turbulent processes. Specifically, we find that the surface density profile is reasonably steep and in the cases considered here, ∼80 per cent of the mass within 50 au is located inside 10–20 au. The quasi-steady mass accretion rate depends strongly on the disc mass and on the mass of the central star. For a constant star to disc mass ratio, however, the relationship between mass accretion rate and central star mass is similar to that found observationally. We further show that the secular evolution of the disc does not typically result in *any* regions that would be unstable to fragmentation, with the region inside 10–20 au being particularly stable unless some mechanism – such as convection (Boss 2004) – can significantly increase the cooling rate.

Our focus in this paper is on the outer cool regions of protoplanetary discs, and for this reason and for simplicity we consider disc models in which self-gravity provides the sole source of angular momentum transport. Of course, both the extreme inner region (inside 0.1 au) and the upper layers of the disc further out could become sufficiently ionized for the MRI to operate (Gammie 1996), and this would modify our results and admit new physical effects. In particular, a pile-up of material brought to within 1–2 au by self-gravity could eventually trigger the onset of the MRI and episodic outbursts (Armitage, Livio & Pringle 2001; Zhu, Hartmann & Gammie 2009). These might be related to the FU Orionis phenomenon (Hartmann & Kenyon 1996). Ultimately the evolution of discs around very young stars could be driven by both MRI and the gravitational instability (Terquem 2008).

The paper is organized as follows. In Section 2, we describe how we can self-consistently model protostellar discs evolving through self-gravity alone. In Section 3, we describe our results, and in Section 4 we summarize our conclusions.

## 2 DISC MODELS

We model the evolution of a self-gravitating protoplanetary disc under the assumptions that the potential is fixed, the disc is in thermal equilibrium at all radii and the local strength of angular momentum transport is set by self-gravity.

### 2.1 Viscous evolution

The surface density $\Sigma(r,t)$ of an axisymmetric disc evolves according to (Lynden-Bell & Pringle 1974; Pringle 1981)

$$\frac{\partial \Sigma}{\partial t} = \frac{3}{r}\frac{\partial}{\partial r}\left[r^{1/2}\frac{\partial}{\partial r}(\nu \Sigma r^{1/2})\right], \tag{1}$$

where $\nu$ is the kinematic viscosity. If the disc is able to attain a steady-state, this equation can be integrated to give an expression for the mass accretion rate $\dot{M}$ which, at radii large compared to the radius of the star, is (Pringle 1981)

$$\dot{M} = 3\pi\nu\Sigma. \tag{2}$$

The steady-state radial surface density profile is therefore determined by the radial profile of the viscosity. We adopt the $\alpha$ formalism (Shakura & Sunyaev 1973) in which the viscosity is taken to be $\nu = \alpha c_s H$, where $c_s$ is the disc sound speed, $H = c_s/\Omega$ is the disc scale height and $\alpha \ll 1$ is a parameter that determines the efficiency of angular momentum transport.

The strength of self-gravity depends upon the thermal properties of the disc. In thermal equilibrium, the viscosity generates dissipation in the disc at a rate $D(R)$ per unit area per unit time, where (Bell & Lin 1994)

$$D(R) = \frac{9}{4}\nu\Sigma\Omega^2, \tag{3}$$

which must balance cooling via thermal emission from the disc surfaces (if the disc is optically thick) or via optically thin emission integrated vertically through the disc.

### 2.2 Determination of $\alpha$

An accretion disc can become gravitationally unstable if (Toomre 1964)

$$Q = \frac{c_s \kappa}{\pi G \Sigma} \sim 1, \tag{4}$$

where $\kappa$ is the epicyclic frequency which is replaced by the angular frequency, $\Omega$, in a Keplerian disc. One possible outcome is that unstable discs fragment to produce bound objects and has been suggested as a possible mechanism for forming giant planets (Boss 1998, 2002). For axisymmetric instabilities, this requires $Q < 1$, while for non-axisymmetric instabilities this can occur for $Q$ values as high as 1.5–1.7 (Durisen et al. 2007). It has, however, been realized recently that the above condition is not sufficient to guarantee fragmentation. The disc must also be able to lose the energy generated by the instability (Gammie 2001; Rice et al. 2003). The rate at which energy must be lost depends on the equation of state (Rice, Lodato & Armitage 2005), but in protostellar discs, the cooling time would generally need to satisfy $t_{\rm cool} \leq 3\Omega^{-1}$ (Gammie 2001).

For cooling times greater than that required for fragmentation, the disc will settle into a quasi-steady state in which the instability acts to transport angular momentum (Laughlin & Rocyzka 1996; Gammie 2001; Lodato & Rice 2004). In principle, this transport need not be local (Balbus & Papaloizou 1999), and if this were the case then neither writing $\alpha$ as a function of local conditions nor using equation (1) would be valid. Simulations, however, show that the local approximation is surprisingly good at capturing the behaviour of self-gravitating protoplanetary discs, which *can* therefore be regarded as having an effective viscosity of the form $\nu = \alpha c_s H$. Moreover, under conditions of thermal equilibrium, the value of $\alpha$ can be derived via a simple energy balance requirement.

The disc cools at a rate (Pringle 1981; Johnson & Gammie 2003)

$$\Lambda = 2\sigma T_{\rm e}^4, \tag{5}$$

where $\sigma$ is the Stefan–Boltzmann constant, $T_{\rm e}$ is the effective temperature and the factor of 2 comes from the radiation escaping on both sides of the disc. If the disc is optically thick, radiation transport can be treated in the diffusion approximation, and the effective temperature can be shown to be given by (Hubeny 1990)

$$T_{\rm e}^4 = \frac{8}{3}\frac{T_{\rm c}^4}{\tau}, \tag{6}$$

where $T_{\rm c}$ is the temperature of the disc midplane and $\tau$ is the Rosseland mean optical depth. The internal energy per unit area, $U$,

is then

$$U = \frac{c_s^2 \Sigma}{\gamma(\gamma - 1)}, \tag{7}$$

where $\gamma$ is the specific heat ratio.

The cooling time is then simply $t_{\rm cool} = U/\Lambda$, where $\Lambda$ is the cooling function given by equation (5). Since we are assuming that the disc is in a quasi-steady state, the cooling must be balanced by dissipation. If we assume that the energy is dissipated locally, which appears to be the case for $Q \sim 1$ (Balbus & Papaloizou 1999; Lodato & Rice 2004), we can use equation (3) to get (Gammie 2001)

$$\alpha = \frac{4}{9\gamma(\gamma - 1) t_{\rm cool} \Omega}. \tag{8}$$

We should acknowledge that the nature of the transport – whether local or global – may depend on the form of the cooling (Mejia et al. 2005; Durisen et al. 2007) and that our use of the local approximation is clearly a simplification. There may well be situations in which the energy is not dissipated locally and although the disc as a whole may be in thermal equilibrium, equation (8) is not strictly valid.

### 2.3 Modelling a fully self-gravitating disc

To consider the evolution of a disc in which angular momentum transport is governed by self-gravity alone, we assume that the disc settles into a quasi-steady state and that energy is dissipated locally. We assume that in this quasi-steady state the Toomre $Q$ parameter satisfies $Q = 1.5$, unless $T_{\rm c} < 10\,{\rm K}$ in which case we set $T_{\rm c} = 10\,{\rm K}$. For a given surface density, equation (4) can be used to determine the midplane sound speed, $c_{\rm s}$. The midplane temperature can then be determined using

$$T_{\rm c} = \frac{\mu m_{\rm p} c_{\rm s}^2}{\gamma k_{\rm B}}, \tag{9}$$

where $\mu = 2.4$ is the mean molecular weight, $m_{\rm p}$ is the proton mass and $k_{\rm B}$ is Boltzmann's constant.

For a given surface density, $\Sigma$, and using the assumption that $Q = 1.5$ (unless $T < 10\,{\rm K}$), we can now determine the midplane temperature. To determine the cooling rate, however, we need to determine the effective temperature, $T_{\rm e}$, for which we need the optical depth. We can approximate the optical depth using

$$\tau = \int_0^\infty {\rm d}z \kappa\left(\rho_z, T_z\right) \rho_z \approx H \kappa\left(\bar{\rho}, \bar{T}\right) \bar{\rho}, \tag{10}$$

where $\kappa$ is the Rosseland mean opacity and $\bar{\rho}$ and $\bar{T}$ are an average density and temperature for which we use $\bar{\rho} = \Sigma/(2H)$ and $\bar{T} = T_{\rm c}$. For the Rosseland mean opacities, we use the analytic approximations from Bell & Lin (1994). Fig. 1 shows the opacity against temperature for a range of densities. The opacity is dominated, in order of increasing temperature, by ice grains, metal grains, molecules, $H^-$ scattering, bound–free and free–free absorption, and electron scattering. The sudden changes in opacity at $T \approx 170$ and $\approx$1000 K are due to the evaporation of the ice mantles on the ices grains and the evaporation of the metal grains, respectively.

Once the optical depth, $\tau$, is known, the cooling function, $\Lambda$, is calculated using a modified form of equations (5) and (6):

$$\Lambda = \frac{16\sigma}{3}\left(T_{\rm c}^4 - T_o^4\right)\frac{\tau}{1 + \tau^2} \tag{11}$$

where $T_o = 10$K is assumed to come from some background source that prevents the midplane cooling below this value (Stamatellos et al. 2007b), and the last term is introduced to smoothly interpolate between optically thick and optically thin regions (Johnson & Gammie 2003). The cooling time is then $t_{\rm cool} = U/\Lambda$ with $U$ given by equation (7) and the viscous $\alpha$ can then be determined using equation (8). The viscosity is then $\nu = \alpha c_{\rm s} H$ and the disc is evolved using equation (1).

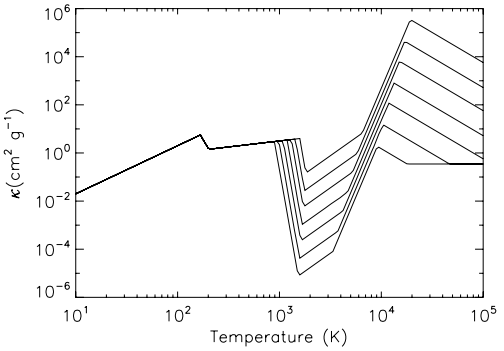


**Figure 1.** Opacities from Bell & Lin (1994) against temperature for densities of $\rho = 10^{-9}, 10^{-8}, 10^{-7}, 10^{-6}, 10^{-5}, 10^{-4}, 10^{-3}\,{\rm g\,cm^{-3}}$.

## 3 RESULTS

### 3.1 Surface density profiles

The simulations presented here assume, initially, a rather extreme case of a central star with a mass of $0.35\,{\rm M}_\odot$ surrounded by a circumstellar disc with a mass of $0.35\,{\rm M}_\odot$. The disc is assumed to have an initial power-law surface density profile $\Sigma \propto r^{-\beta}$ between 0.5 and 50 au. The assumption that $Q = 1.5$ then determines the disc midplane temperature, $T_{\rm c}$, with the additional constraint that $T_{\rm c} \geq 10\,{\rm K}$. The process described above determines $\alpha$ and the disc is then evolved in time using equation (1). We consider three different initial surface density profile, $\beta = 2.0$, 1.5 and 1.0.

The surface density evolution for the three initial profiles is shown in Fig. 2. We should stress that we do not assume that the initial profiles are necessarily realistic, but simply want to establish if such discs will settle into quasi-steady states, and if such a state depends in any way on the initial surface density profiles. Each panel in Fig. 2 shows the initial power-law surface density, four subsequent surface density profiles each separated by 20 000 years and the final surface density (dashed-line) at the end of the simulation which we stop after $10^6$ years. What this shows is that the surface density adjusts in all three cases to a state that appears to be largely independent of the initial surface density profile. For $\beta = 1.0$ and 1.5, this settling takes some time ($\sim$80 000 years), while for $\beta = 2$, it occurs almost immediately. For clarity, Fig. 3 shows the surface density profile when a quasi-steady state has just been achieved (solid line). With time, this profile moves inwards and the disc mass decreases, as illustrated by the dashed line in Fig. 3 which shows the surface density profile when $M_{\rm disc} = 0.25\,{\rm M}_\odot$.

In all cases, what is happening is that mass is redistributing itself to produce a state in which the accretion rate, $\dot{M}$, is largely independent of $r$. The is illustrated in Fig. 4 which shows the evolution of the mass accretion rate for $\beta = 1.5$. The behaviour is essentially the same for $\beta = 1$ and 2 except that the latter reaches an approximately constant mass accretion rate more rapidly than the other two cases. In the prescription presented here, the viscous $\alpha$ depends on the local cooling rate – which depends on the local temperature – and the accretion rate depends on the local viscosity and surface

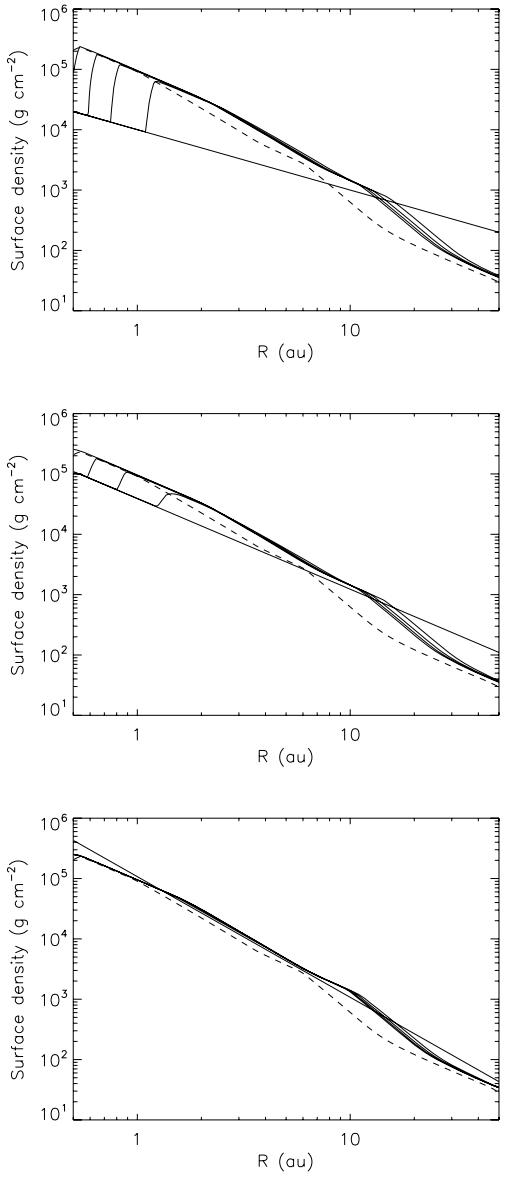


**Figure 2.** Figure showing how 0.35 $M_\odot$ discs around a 0.35 $M_\odot$ star with initial surface density profiles of $\Sigma \propto r^{-1}$ (top panel), $\Sigma \propto r^{-1.5}$ (middle panel) and $\Sigma \propto r^{-2}$ (bottom panel) evolve into quasi-steady states. In all the cases, the resulting quasi-steady profiles are the same.

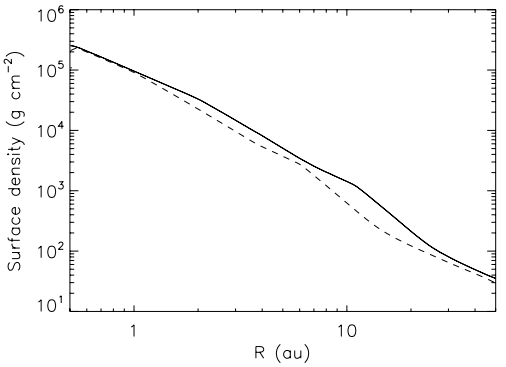


**Figure 3.** Figure showing the quasi-steady surface density profile for a 0.35 $M_\odot$ disc around a 0.35 $M_\odot$ star (solid line). The profile moves inwards with time (dashed line) as mass accretes on to the central star.

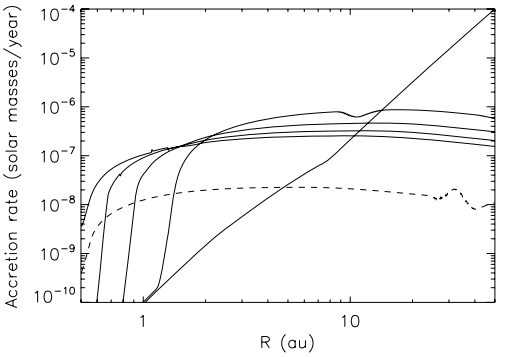


**Figure 4.** Figure showing the mass accretion rate against radius at different times for $\Sigma \propto r^{-1.5}$. The almost diagonal line shows the initial mass accretion rate while the other solid lines show the accretion rate at 20 000 years intervals until a quasi-steady rate is achieved with a mass accretion rate of $\dot{M} \sim 10^{-7}\,M_\odot\,yr^{-1}$. The dashed line shows the accretion rate after $10^6$ years when the disc mass has decreased to 0.25 $M_\odot$. The two other initial surface density profiles (which we do not show here) evolve to the same quasi-steady accretion rate, but over slightly different time-scales, with the $\Sigma \propto r^{-2}$ disc evolving to a quasi-steady state much more rapidly than $\Sigma \propto r^{-1}$ and $\Sigma \propto r^{-1.5}$ discs.

density (e.g. equation 2). For initially flatter surface density profiles ($\Sigma \propto r^{-1}$ and $\Sigma \propto r^{-1.5}$), the outer disc contains most of the mass. To be gravitationally stable (see equation 4), the temperature in the outer disc also needs to be high. The inner disc, on the other hand, can have relatively low temperatures and remain gravitationally stable. The cooling time, and consequently viscosity, in the outer disc is therefore significantly greater than in the inner disc, producing an initially much larger mass accretion rate in the outer disc than in the inner disc. This process, however, moves mass inwards and in doing so not only increases the surface density in the inner disc but also the temperature to keep the disc gravitationally stable. This increases the cooling rate in the inner disc, the viscosity and the mass accretion rate. Eventually, the mass is redistributed such that the entire disc has the same mass accretion rate. If the initial surface density profile is, however, initially close to the quasi-steady profile – as in the third panel of Fig. 2 – very little redistribution is required and the disc very quickly settles into a quasi-steady state.

This mass redistribution leads to quasi-steady surface density profiles that are reasonably steep ($\Sigma \sim r^{-2}$) and that have quite a substantial break at 10–20 au. Even though the discs extend to 50 au, most of the mass (>80 per cent) is actually located in the inner disc. It is now generally accepted that discs disappear within a few million years (Haisch, Lada & Lada 2001) and consequently gas giant planets need to form within this time-scale. A substantial reservoir of mass in the inner disc could significantly accelerate planet growth if gaseous planets form via the standard core accretion scenario (Pollack et al. 1996). This type of profile is also qualitatively consistent with observations of massive discs (Rodriguez et al. 2005; Carrasco-Gonzalez et al. 2009) that suggest that such discs have small radii ($r_{\rm disc} \sim 25$ au). It is also quite likely that with so much mass located in the optically thick inner regions, and the sub-mm flux largely determined by the cold, outer disc, the masses of such discs could be easily underestimated (Hartmann et al. 2006). Such gas rich inner disc could be detected using near-IR gas emission lines such as the CO bandhead (Thi et al. 2005; Najita et al. 2007). However, for the disc masses considered here, these lines are still

optically thick and will still not provide accurate probes of the disc mass.

Although the goal here is to illustrate the quasi-steady structure of a self-gravitating disc, it is also interesting to consider the time evolution of these systems. First, since the quasi-steady surface density profile is independent of the initial conditions, continuing these simulations to $10^6$ years allows us to compare the quasi-steady nature for different disc masses. There is also no reason to suspect that the mass falling on to the disc will do so in such a way as to immediately produce a quasi-steady disc. We might therefore expect that the disc will not initially be in equilibrium. The settling times achieved here ($<10^5$ years) are similar to and probably less than typical free-fall times (Ward-Thompson et al. 2007), suggesting that these systems could quite quickly attain quasi-steady states. Fig. 2 also shows that beyond $\sim$1 au, the disc reaches a quasi-steady state in 20 000 years or less and might imply that these systems are rarely out of equilibrium.

### 3.2 Temperature profiles

The evolution of the midplane temperature is shown in Fig. 5. Again, the figure shows the initial temperature profile followed by four subsequent temperature profiles separated by 20 000 years, and a final temperature profile (dashed line) after $10^6$ years. Since the temperature is specified using $Q = 1.5$ and $T_c \geq 10$ K, and since the quasi-steady profiles are essentially the same in all cases, we show only the temperature profile for $\Sigma \propto r^{-1.5}$. From Figs 1 and 5, we can start to understand the disc structure. The outer disc has $T_c <$ 170 K and so the opacity is dominated by ice grains. The asymptotic nature of the temperature profile at large radii is simply due to the assumption that $T_c \geq 10$ K. The change in slope at, initially, a radius between 10 and 20 au that moves inwards with time is due to the evaporation of the ice mantles on the grains and is essentially the 'snowline'. The opacity of the inner part of the disc (within $\sim$10 au) is dominated by metal grains until the temperature reaches 1000–2000 K where the grains evaporate and the temperature cannot rise significantly due to the sudden decrease in opacity. This results in a further change in the surface density profile. The quasi-steady nature is therefore quite strongly dependent on the opacity of the disc material. In the vertically averaged approximation, the optical depth is evaluated using only the midplane value of the opacity. In the hot inner regions where the midplane temperature exceeds the dust sublimation temperature, this is likely to result in an underestimation of the true optical depth, since the surface regions are cooler and could have a larger opacity. To evaluate the true optical depth in detail would require solving for the vertical structure and considering the time-scales for the evaporation and condensation of particulates within the turbulent flow, which we do not attempt. Clearly, however, the sense of the effect will be to increase the optical depth and cooling time still further and hence the disc temperature at the midplane will remain above the grain evaporation temperature.

As will be discussed in more detail later, the $\alpha$ values in the inner regions of these discs are low and, as shown in Fig. 8, within $\sim$3 au are $<10^{-4}$. It is often assumed that $\alpha \sim 10^{-2}$ which, for mass accretion rates similar to those shown here, would imply much lower temperatures in the inner disc. Crystalline silicates – which are commonly observed in protostellar discs (Bouwman et al. 2001; van Boekel et al. 2004) and require $T > 800$ K – are therefore generally thought to form close to the central star ($r \sim 0.1$ au for TTauri stars) (Dullemond, Apai & Walch 2006) and then transported outwards via turbulent mixing to at least 10–20 au (Gail 2001). Fig. 5, however, suggests that when the transport processes are dominated by self-gravity, the temperature could be high enough to form crystalline silicates at radii of a few astronomical units.

### 3.3 Mass accretion

As discussed above (and illustrated in Fig. 4), the disc relatively quickly settles into a quasi-steady state with an approximately constant mass transfer rate. The corresponding $\alpha$ values are shown in Fig. 6. Again this figure shows the initial $\alpha$ profile, four subsequent $\alpha$ profiles separated by 20 000 years, and the final $\alpha$ profile after $10^6$ years. The strong dependence of $\alpha$ on the midplane temperature means that small variations in $T_c$ can produce large variations in $\alpha$. This only really occurs in the outer disc when $T_c$ is close to the minimum temperature of 10 K, or where opacity changes produce sudden changes in $T_c$ coupled with the initial conditions being far from

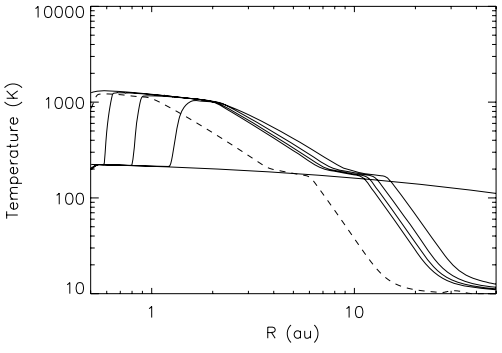


**Figure 5.** Disc Midplane temperature against radius for $\Sigma \propto r^{-1.5}$. The temperature profiles for $\Sigma \propto r^{-1}$ and $\Sigma \propto r^{-2}$ are not shown since the quasi-steady profiles are the same. The figure shows the initial temperature profile followed by four profiles separated by 20 000 years, and the profile after $10^6$ years (dashed line). The form of the temperature profile is essentially determined by the opacity. Beyond 10 au, ice grains dominate the opacity. These melt at 170 K, producing the change in profile at $\sim$10 au. Within 10 au, metal grains dominate the opacity until the temperature reaches 1000–2000 K at which point these grains evaporate.

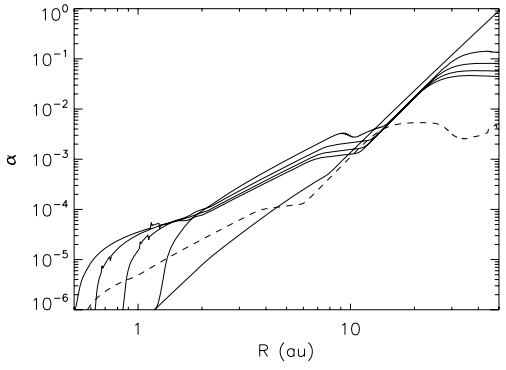


**Figure 6.** Viscous $\alpha$ against radius at different times for $\Sigma \propto r^{-1.5}$. The results for $\Sigma \propto r^{-1}$ and $\Sigma \propto r^{-2}$ are essentially the same, so are not shown. The figure shows the initial $\alpha$ profile followed by four $\alpha$ profiles separated by 20 000 years (solid lines) until a quasi-steady state, and the $\alpha$ profile after $10^6$ years (dashed line). It has been shown that fragmentation can occur if $\alpha \sim 0.06$. The $\alpha$ values in the inner disc can be very small, well below that required for fragmentation. The $\alpha$ value in the outer disc can, however, become quite large ($>10^{-2}$) but in this case is still below – but close to – that required for fragmentation.

the equilibrium conditions. The $\alpha$ and $\dot{M}$ profiles have therefore been averaged to remove these small-scale variations. What Fig. 6 illustrates is that the $\alpha$ value in a quasi-steady, self-gravitating disc is not constant and can reach extremely low-values in the inner disc. In a more complete model, other sources of transport (such as weak turbulence in the disc mid-plane excited by MRI active zones at the disc surface) might well dominate in this region. Such a process could also result in episodic accretion events if the other source of transport were to depend on the disc properties – such as temperature in the case of MRI – and could explain phenomena such as FU Orionis outbursts (Hartmann & Kenyon 1996). The mass accretion rate *into* the inner disc and ultimately on to the star, however, would still be set by the self-gravitating transport taking place at larger radii (Boley & Durisen 2008).

Fig. 4 also shows that for our chosen parameters ($M_* = 0.35\,\mathrm{M}_\odot$ and $M_{\rm disc} = 0.35\,\mathrm{M}_\odot$) the initial quasi-steady mass accretion rate is $\sim 2 \times 10^{-7}\,\mathrm{M}_\odot\,\mathrm{yr}^{-1}$. The dashed line in Fig. 4 shows the accretion rate after $10^6$ years. At this stage, the disc mass is $\sim 0.25\,\mathrm{M}_\odot$ and the accretion rate is $\sim 10^{-8}\,\mathrm{M}_\odot\,\mathrm{yr}^{-1}$. Since this is the quasi-steady rate for a $0.25\,\mathrm{M}_\odot$ disc around a $0.35\,\mathrm{M}_\odot$ star, this illustrates that the accretion rate depends non-linearly on the disc mass (a factor of 1.4 reduction in disc mass reduces the accretion rate by about an order of magnitude).

This dependence of the quasi-steady accretion rate on the disc mass can be roughly understood by considering the method discussed in Section 2. For a constant Toomre stability parameter, $Q$, and central mass, the sound speed, $c_{\rm s}$, depends linearly on the surface density. Since $c_{\rm s} \propto \sqrt{T_{\rm c}}$, this gives $T_{\rm c} \propto \Sigma^2$. Using $\nu = \alpha c_{\rm s}^2/\Omega$, the mass accretion rate – shown in equation (2) – can be rewritten as $\dot{M} \propto \alpha\Sigma^3$. Combining equations (7), (8), (10) and (11), and using $\tau \approx \kappa\,\Sigma$, gives $\alpha \propto \Sigma^4$ and consequently $\dot{M} \propto \Sigma^7$. Here, for simplicity, we ignore $T_o$ in equation (11) and assume that the disc is optically thick so $\tau/(1+\tau^2) \approx \tau$. As $\Sigma$ is essentially determined by the disc mass, the accretion rate then depends on the disc mass to the seventh power. A factor of 1.4 reduction in disc mass would produce an order of magnitude change in accretion rate, consistent with that shown in Fig. 4.

### 3.4 Fragmentation

It has been shown (Gammie 2001; Rice et al. 2003) that there is a minimum cooling time, $t_{\rm cool}$, for which a self-gravitating disc can remain in a quasi-steady state without fragmenting to form bound objects. The exact value of the minimum cooling time depends on the equation of state (Rice et al. 2005) with fragmentation occurring for $t_{\rm cool} \leq 3\Omega^{-1}$ when the specific heat ratio $\gamma = 5/3$ (Gammie 2001). Rice et al. (2005), however, show that for all values of $\gamma$ the fragmentation boundary occurs for $\alpha \sim 0.06$. Fig. 6 shows that once the disc settles into a quasi-steady state, the $\alpha$ values in the inner disc ($r < 10\,\mathrm{au}$) are well below that required for fragmentation. Between 20 and 50 au, however, $\alpha$ is almost constant and has a value ($\alpha \sim 0.04$) just below that required for fragmentation. A small increase in disc mass would, however, increase $\alpha$ and could produce conditions that would allow for fragmentation in the outer parts of such discs (Stamatellos, Hubber & Whitworth 2007a; Greaves et al. 2008). We should, however, add that the results obtained by Gammie (2001) and Rice et al. (2003) were for systems in which the cooling time was chosen to be the same at all radii. Mejia et al. (2005) argue that in systems with a radially varying cooling time, the fragmentation boundary may not be a simple function of cooling time and that there could be regions with $\alpha > 0.06$ that do not fragment.

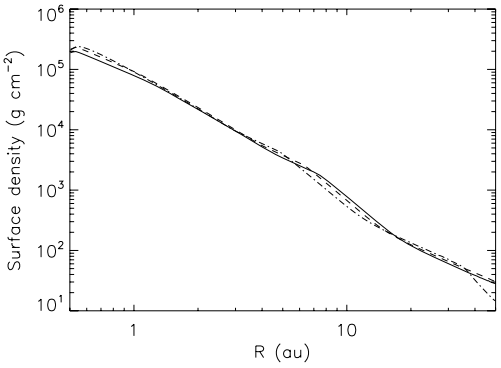


**Figure 7.** Quasi-steady surface density profiles for $M_{\rm disc} = 0.25\,\mathrm{M}_\odot$ and $M_* = 0.25\,\mathrm{M}_\odot$ (solid line), $M_* = 0.35\,\mathrm{M}_\odot$ (dashed line) and $M_* = 0.5\,\mathrm{M}_\odot$ (dash–dot line). The profiles are almost the same, but with a few differences due to the different temperature profiles resulting from the Toomre $Q$ parameter's dependence on the mass of the central star.

### 3.5 Variation with central mass

We have also considered how the mass of the central object influences the quasi-steady nature of a self-gravitating disc. To do this, we consider a disc mass of $0.25\,\mathrm{M}_\odot$ around central objects with masses of $M_* = 0.25$, 0.35 and $0.5\,\mathrm{M}_\odot$. In all cases, we assume an initial surface density profile of $\Sigma \propto r^{-2}$ and evolve the system until a quasi-steady state is reached. The resulting quasi-steady surface density profiles are shown in Fig. 7 with the solid line for $M_* = 0.25\,\mathrm{M}_\odot$, the dashed line for $M_* = 0.35\,\mathrm{M}_\odot$ and the dashed–dot line for $M_* = 0.5\,\mathrm{M}_\odot$. The surface density profiles are, as expected, quite similar. The slight differences are a consequences of the dependence of the Toomre $Q$ parameter on the mass of the central object. This can be understood by considering Fig. 8 which shows the temperature profile for the three cases. Since we assume $Q = 1.5$, as the central object mass decreases (decreasing the orbital frequency $\Omega$) the sound speed, $c_{\rm s}$, and hence temperature, needs to

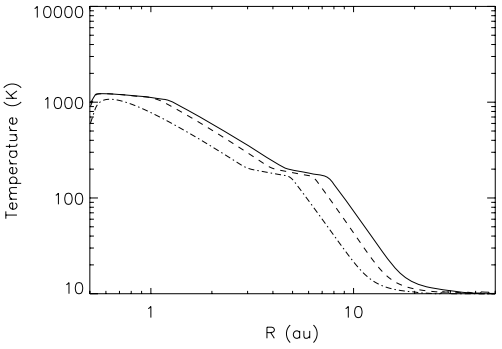


**Figure 8.** Quasi-steady temperature profiles for $M_{\rm disc} = 0.25\,\mathrm{M}_\odot$ and $M_* = 0.25\,\mathrm{M}_\odot$ (solid line), $M_* = 0.35\,\mathrm{M}_\odot$ (dashed line) and $M_* = 0.5\,\mathrm{M}_\odot$ (dash–dot line). The difference in the profiles is a result of the dependence of the Toomre $Q$ on the mass of the central star (through $\Omega$). As the central star mass decreases, the sound speed – and hence temperature – needs to increase to maintain a constant $Q$ value. This means that the radii at which ice mantles and metals evaporate differs for the different central star masses, and produces (as seen in Fig. 7) slightly different surface density profiles.

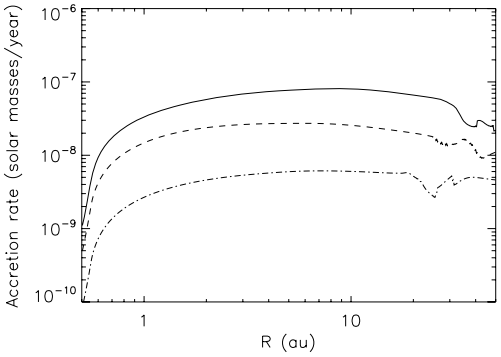


**Figure 9.** Quasi-steady mass accretion rates for $M_{\rm disc} = 0.25\,{\rm M}_\odot$ and $M_* = 0.25\,{\rm M}_\odot$ (solid line), $M_* = 0.35\,{\rm M}_\odot$ (dashed line) and $M_* = 0.5\,{\rm M}_\odot$ (dash–dot line). The accretion rate for $M_* = 0.25\,{\rm M}_\odot$ is significantly greater than for $M_* = 0.5\,{\rm M}_\odot$. This is a consequence of the increased disc temperature required to keep the disc around the lower mass star gravitationally stable. The strong dependence of $\alpha$ on temperature results in the $M_* = 0.25\,{\rm M}_\odot$ system having an accretion rate more than an order of magnitude greater than the $M_* = 0.5\,{\rm M}_\odot$ system.

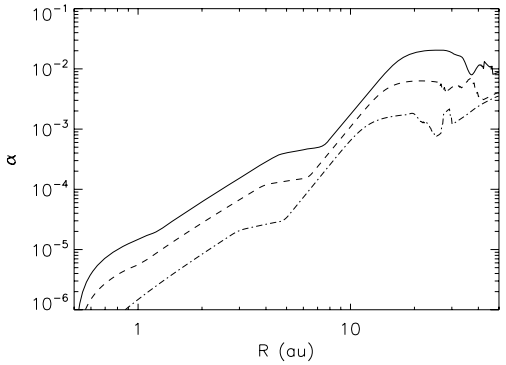


**Figure 10.** Effective viscous $\alpha$ profiles for $M_{\rm disc} = 0.25\,{\rm M}_\odot$ and $M_* = 0.25\,{\rm M}_\odot$ (solid line), $M_* = 0.35\,{\rm M}_\odot$ (dashed line) and $M_* = 0.5\,{\rm M}_\odot$ (dash–dot line). As discussed in the text, for a fixed disc mass $\alpha$ increases with decreasing star mass. In all cases, however, the $\alpha$ values in the inner disc are well below that required for fragmentation. Although larger in the outer disc, the values are close to, but still below, that needed for fragmentation.

increase. This changes the locations where the ice mantles melt and where the metal grains evaporate and hence results in different central object masses producing slightly different – although similar – surface density profiles.

Fig. 9 shows the quasi-steady mass accretion rates for $M_* = 0.25\,{\rm M}_\odot$ (solid line), $M_* = 0.35\,{\rm M}_\odot$ (dashed line) and $M_* = 0.5\,{\rm M}_\odot$ (dash–dot line). There is a very strong dependence on the central mass with the accretion rate for $M_* = 0.25\,{\rm M}_\odot$ being more than an order of magnitude greater than that for $M_* = 0.5\,{\rm M}_\odot$. Again, we can understand this dependence by considering the method described in Section 2. For a constant disc mass, and hence surface density ($\Sigma$), a constant Toomre $Q$ requires $c_{\rm s} \propto 1/\Omega \propto 1/\sqrt{M_*}$ giving $T_{\rm c} \propto 1/M_*$. Using $\nu = \alpha c_{\rm s}^2/\Omega$, the mass accretion rate can be rewritten as $\dot{M} \propto \alpha T_{\rm c}^{3/2}$. Equations (7), (8), (10) and (11) can again be used to show that $\alpha \propto T_{\rm c}^{5/2}$, giving a mass accretion rate of $\dot{M} \propto T_{\rm c}^4$ or $\dot{M} \propto 1/M_*^4$. A factor of 2 increase in the mass of the central star therefore reduces the mass accretion rate by a factor of 22, consistent with that seen in Fig. 9. If, however, we combine this relationship ($\dot{M} \propto 1/M_*^4$) with the relationship between accretion rate and disc mass ($\dot{M} \propto \Sigma^7 \propto M_{\rm disc}^7$), the accretion rate actually increase as $\dot{M} \propto M_*^3$ if a constant disc to star mass ratio is maintained. This is consistent with the observations that in the Orion Nebula cluster massive discs are more common around lower mass stars (Eisner et al. 2008).

Something to point out is that as the disc mass decreases, it becomes increasingly difficult to sustain steady, self-gravitating accretion in the outer regions of the disc. The surface density (Figs 2 and 3) and temperature profiles (Figs 5 and 8) show that most of the mass is in the inner disc and that, as the disc mass decreases, the temperature in the outer disc approaches 10 K, our assumed minimum temperature. Equation (11) shows that as $T_{\rm c}$ approaches 10 K, the cooling function becomes very small, the cooling time becomes very long and the effective $\alpha$ becomes very small. Decreasing the disc mass much below $0.25\,{\rm M}_\odot$ effectively turns off self-gravitating accretion beyond $\sim$30 au. This is, of course, due to our assumption that the quasi-steady Toomre $Q$ value is 1.5. If quasi-steady transport can occur for larger values of $Q$, self-gravitating transport could still operate effectively at lower disc masses. This also has implications for the production of brown dwarfs and low-mass companions at large radii (Stamatellos et al. 2007a), suggesting that fragmentation at large radii is unlikely when the disc is in a quasi-steady state. This does not preclude fragmentation at large radii, but implies that it must either occur when the disc is extremely massive, or must occur when the disc has not yet reached a quasi-steady state.

The corresponding $\alpha$ profiles are shown in Fig. 10. The dependence of $\alpha$ on $M_*$ discussed above gives larger $\alpha$ values for $M_* = 0.25\,{\rm M}_\odot$ than for $M_* = 0.5\,{\rm M}_\odot$. Again the $\alpha$ values in the inner disc are well below those required for fragmentation, while those in outer disc are close to, but below, the required value ($\alpha = 0.06$). As discussed earlier, however, small changes in some of the parameters could produce conditions suitable for fragmentation in the outer parts of the disc, but as suggested by Rafikov (2005), it is extremely difficult to see how fragmentation can occur within 10 au even for the relatively massive discs considered here.

## 4 DISCUSSION AND CONCLUSIONS

We consider here the evolution of protostellar discs in which angular momentum transport is driven only by self-gravity. We are particularly interested in the quasi-steady nature of such systems, which we define here as a state in which the mass accretion rate is approximately the same at all radii. We assume that the disc will cool to a state of marginal gravitational stability ($Q \sim 1.5$) and will then be in thermal equilibrium. The evolution of such systems is determined by the effective gravitational viscosity which is calculated from the assumption that the viscosity dissipates energy at the same rate as energy is lost from the disc via radiative cooling – which depends on the chosen opacity. This is in some sense the inverse of a ' classical' $\alpha$ disc (Shakura & Sunyaev 1973) in which the prescribed $\alpha$ value determines the viscosity, which then sets the dissipation and cooling rates.

We carried out a number of different simulations, initially considering a central object of $0.35\,{\rm M}_\odot$ surrounded by an equal-mass disc with a power-law surface density profile from 0.5 to 50 au. We also considered central masses of 0.25 and $0.5\,{\rm M}_\odot$ with a disc mass of $0.25\,{\rm M}_\odot$. The discs are in all cases evolved until a quasi-steady state is reached. The primary results are summarized below.

(i) The discs reasonably quickly settle into a quasi-steady state that is largely independent of the initial surface density profile. The settling time does depend somewhat on the initial profile, but

beyond ∼1 au a quasi-steady state is reached in 20 000 years or less, suggesting that such systems will rarely be out of equilibrium.

(ii) The quasi-steady surface density profile is relatively steep ($\Sigma \sim r^{-2}$) with changes in profile that correspond to the melting of ice grains (effectively the 'snowline') and the evaporation of metal grains. The steep profile means that most (∼80 per cent) of the mass is located within 10–20 au, even though the discs extend initially to 50 au. Having a lot of the mass in the inner disc could aid planet formation, and is consistent with current observations showing that massive discs have small radii (Rodriguez et al. 2005).

(iii) The corresponding temperature profile indicates that in a quasi-steady state the inner disc (within ∼3 au) can be hot ($T_c > 1000$ K) which suggests that such regions could be sufficiently ionized to be unstable to the growth of MRI (Balbus & Hawley 1991). The MRI viscosity is likely to be significantly larger than the effective gravitational viscosity, so will drain the inner disc, potentially producing FU Orionis-like outbursts (Armitage et al. 2001; Zhu et al. 2009). This process could repeat once the inner disc has been replenished by material from the outer disc. The hot inner disc ($T_c > 800$ K) also suggests that the formation of crystalline silicates could occur at relatively large radii ($r < 3$–4 au) during the earliest stages of star formation.

(iv) The mass accretion rate in quasi-steady discs also has a strong dependence on disc mass and on the mass of the central star. From the simulations, and from analytic approximations, we find $\dot{M} \propto \Sigma^7 \propto M_{\rm disc}^7$ and $\dot{M} \propto 1/M_*^4$. Together this suggests that for a constant disc to star mass ratio $\dot{M} \propto M_*^3$, consistent with suggestions (Kratter, Matzner & Krumholz 2008) that the gravitational instability is the most important mechanism for stars with final masses $>1\,{\rm M}_\odot$. This is also intriguingly similar to the $\dot{M} \propto M_*^2$ relationship between accretion rate and stellar mass determined observationally (Muzerolle et al. 2005), although the simulation results probably apply to systems considerably younger than those observed.

(v) It has been shown (Gammie 2001; Rice et al. 2003) that fragmentation requires rapid cooling and is equivalent to $\alpha \leq 0.06$ (Rice et al. 2005). Despite the discs considered here being massive, none of the quasi-steady discs had $\alpha > 0.06$ at any radii. In the outer disc ($r > 20$ au), the $\alpha$ value was close to the fragmentation limit, but in the inner disc it was orders of magnitude below that required. Small changes in some disc properties could lead to fragmentation conditions at large radii (Stamatellos et al. 2007a; Greaves et al. 2008), but this does not appear to be possible in the inner disc, consistent with other calculations (Rafikov 2005, 2007; Whitworth & Stamatellos 2006). The quasi-steady surface density profile also has most of the mass in the inner disc, suggesting that if discs do fragment at large radii, they either do so prior to settling into a quasi-steady state or do so when the disc is extremely massive.

Overall, the results presented here suggest a scenario in which – while mass is falling from the envelope on to the disc – the disc mass remains comparable to the central star mass and the system evolves towards a quasi-steady state with mass accretion rates in excess of $10^{-7}\,{\rm M}_\odot\,{\rm yr}^{-1}$. MHD turbulence (MRI) will probably also play a role in some regions of the disc (Armitage et al. 2001; Terquem 2008) and, in particular, could lead to FU Orionis outbursts if the inner disc temperature exceeds ∼1400 K (Armitage et al. 2001; Zhu et al. 2009). Once envelope infall ceases, the disc mass will start to decrease, rapidly reducing the mass accretion rate due to self-gravity. The midplane in the inner disc will have a very low viscosity ($\alpha < 10^{-4}$) and will effectively become dead. This can occur for relatively large disc masses ($M_{\rm disc} \sim 0.1\,{\rm M}_\odot$) which, together with most of the mass being in the inner disc, could enhance planet formation. The low viscosities in the midplane of the inner disc also means that embedded planets can easily clear a large inner gap (Syer & Clarke 1995) and could explain some of the observed systems with near-IR deficits (Hartmann 2008), often referred to as transition systems.

## ACKNOWLEDGMENTS

PJA acknowledges support from the NSF (AST-0807471), from NASA's Origins of Solar Systems program (NNX09AB90G) and from NASA's Astrophysics Theory and Fundamental Physics program (NNX07AH08G). WKMR acknowledges support from the Scottish Universities Physics Alliance (SUPA). The authors would also like to acknowledge useful discussions with Lee Hartmann and Dick Durisen, and would like to thank the referees for their constructive comments.

## REFERENCES

Armitage P. J., Livio M., Pringle J. E., 2001, MNRAS, 324, 705
Balbus S. A., Hawley J. F., 1991, ApJ, 376, 214
Balbus S. A., Papaloizou J. C. B., 1999, ApJ, 521, 650
Bell K. R., Lin D. N. C., 1994, ApJ, 427, 987
Blaes O. M., Balbus S. A., 1994, ApJ, 421, 163
Boley A. C., Durisen R. H., 2008, ApJ, 685, 1193
Boley A. C., Mejía A. C., Durisen R. H., Cai K., Pickett M. K., D'Alessio P., 2006, ApJ, 651, 517
Boss A. P., 1998, ApJ, 503, 923
Boss A. P., 2002, ApJ, 576, 462
Boss A. P., 2004, ApJ, 610, 456
Bouwman J., Meeus G., de Koter A., Hony S., Dominik C., Waters L. B. F. M., 2001, A&A, 375, 950
Carrasco-Gonzalez C., Rodriguez L. F., Anglada G., Curiel S., 2009, ApJ, 693, L86
Caselli P., Benson P. J., Myers P. C., Tafalla M., 2002, ApJ, 572, 238
Eisner J. A., Plambeck R. L., Carpenter J. M., Corder S. A., Qi C., Wilner D., 2008, ApJ, 683, 304
Dullemond C. P., Apai D., Walch S., 2006, ApJ, 640, L67
Durisen R. H., Boss A. P., Mayer L., Nelson A. F., Quinn T., Rice W. K. M., 2007, in Reipurth B., Jewitt D., Keil K., eds, Protostars and Planets V. Univ. of Arizona Press, Tucson, p. 701
Forgan D., Rice K., Stamatellos D., Whitworth A., 2009, MNRAS, 394, 882
Gail H.-P., 2001, A&A, 378, 192
Gammie C. F., 1996, ApJ, 457, 355
Gammie C. F., 2001, ApJ, 553, 174
Greaves J. S., Richards A. M. S., Rice W. K. M., Muxlow T. W. B., 2008, MNRAS, 391, L74
Haisch K. E., Lada E. A., Lada C. J., 2001, AJ, 121, 2065
Hartmann L., 2008, Phys. Scr., 130, 014012
Hartmann L., Kenyon S. J., 1996, ARA&A, 34, 207
Hartmann L., D'Alessio P., Calvet N., Muzerolle J., 2006, ApJ, 648, 484
Hubeny I., 1990, ApJ, 351, 632
Johnson B. M., Gammie C. F., 2003, ApJ, 597, 131
Kratter K. M., Matzner C. D., Krumholz M. R., 2008, ApJ, 681, 375
Laughlin G., Bodenheimer P., 1994, ApJ, 436, 335
Laughlin G., Rozycka M., 1996, ApJ, 456, 279
Lin D. N. C., Pringle J. E., 1987, MNRAS, 225, 607
Lodato G., Rice W. K. M., 2004, MNRAS, 351, 630
Lodato G., Rice W. K. M., 2005, MNRAS, 358, 1489
Lynden-Bell D., Pringle J. E., 1974, MNRAS, 168, 603
Matzner C. D., Levin Y., 2005, ApJ, 628, 817
Mejía A. C., Durisen R. H., Pickett M. K., Cai K., 2006, ApJ, 619, 1098
Muzerolle J., Luhmann K. L., Briceño C., Hartmann L., Calvet N., 2005, ApJ, 625, 906

Najita J. R., Carr J. S., Glassgold A. E., Valenti J. A., 2007, in Reipurth B., Jewitt D., Keil K., eds, Protostars and Planets V. Univ. of Arizona Press, Tucson, p. 507
Papaloizou J. C. B., Nelson R. P., 2003, MNRAS, 339, 983
Pollack J. C. B., Hubickyj O., Bodenheimer P., Lissauer J. J., Podolak M., Greenzweig Y., 1996, Icarus, 124, 62
Pringle J. E., 1981, ARA&A, 19, 137
Rafikov R. R., 2005, ApJ, 621, L69
Rafikov R. R., 2006, ApJ, 648, 666
Rice W. K. M., Armitage P. J., Bate M. R., Bonnell I. A., 2003, MNRAS, 339, 1025
Rice W. K. M., Lodato G., Armitage P. J., 2005, MNRAS, 364, L56
Rodriguez L. F., Loinard L., D'Alessio P., Wilner D. J., Ho P. T. P., 2005, ApJ, 621, L133
Shakura N. I., Sunyaev R. A., 1973, A&A, 24, 337
Stamatellos D., Whitworth A. P., 2008, A&A, 480, 879
Stamatellos D., Whitworth A. P., 2009, MNRAS, 392, 413
Stamatellos D., Hubber D. A., Whitworth A. P., 2007a, MNRAS, 382, L30
Stamatellos D., Whitworth A. P., Bisbas T., Goodwin S., 2007b, A&A, 475, 37
Syer D., Clarke C., 1995, MNRAS, 277, 758
Terebey S., Shu F. H., Cassen P., 1984, ApJ, 286, 529
Terquem C. E. J. M. L. J., 2008, ApJ, 689, 532
Thi W.-F., van Dalen B., Bik A., Waters L. B. F. M., 2005, A&A, 430, L61
Toomre A., 1964, ApJ, 139, 1217
van Boekel R. et al., 2004, Nat, 432, 479
Vorobyov E. I., Basu S., 2007, MNRAS, 381, 1009
Ward-Thompson D., André P., Crutcher R., Johnstone D., Onishi T., Wilson C., 2007, in Reipurth B., Jewitt D., Keil L., eds, Protostars and Planets V. Univ. of Arizona Press, Tucson, p. 33
Whitworth A. P., Stamatellos D., 2006, A&A, 458, 817
Zhu Z., Hartmann L., Gammie C. F., 2009, ApJ, 694, 1045

This paper has been typeset from a TEX/LATEX file prepared by the author.